POLITECNICO DI TORINO
Repository ISTITUZIONALE

Non-intrusive Uncertainty Propagation in the ARC Fusion Reactor through the nemoFOAM Multi-physics Tool

(Article begins on next page)

11 February 2024

Non-intrusive Uncertainty Propagation in the ARC Fusion Reactor through the nemoFOAM Multi-physics Tool

A. Aimetta, M. Caravello, N. Abrate, S. Dulla and A. Froio

Politecnico di Torino, Dipartimento Energia, NEMO group
Corso Duca degli Abruzzi, 24 - 10129 Torino (Italy)

alex.aimetta@polito.it

ABSTRACT

In the framework of the multiphysics analysis of nuclear reactors, it is important to assess the impact of nuclear data uncertainties on relevant thermal-hydraulic quantities like temperature, pressure and mass flow rate. This is particularly important for the safety assessment and for the design verification of fission and fusion systems, through the so-called Best Estimate Plus Uncertainty approach, which qualifies the outputs providing an estimate of their uncertainties. In this work, the uncertainties are propagated from the nuclear data libraries to the thermal-hydraulic quantities of the Breeding Blanket of the Affordable, Robust, Compact fusion reactor thanks to the multiphysics tool *nemoFOAM*, and employing different uncertainty propagation techniques, like the Total Monte Carlo and the Unscented Transform.

KEYWORDS: Multiphysics; Uncertainty Propagation; Reduced Order Models; Nuclear Fusion

1. INTRODUCTION

The Affordable, Robust, Compact (ARC) reactor is a fusion reactor design developed at the Massachusetts Institute of Technology (MIT) [1], which will demonstrate the possibility to produce electrical power (250 MW$_e$) using High-Temperature Superconductor magnets and a fully liquid breeding blanket made of the FLiBe molten salt (76.79% fluorine, 9.09% beryllium and 14.12% lithium). This salt, in principle, would allow to breed a sufficient quantity of tritium so that ARC can be self-sustaining from the point of view of the fuel (i.e. Tritium Breeding Ratio (TBR) larger than 1), to moderate and shield the neutrons from the D-T plasma reactions and to extract the power deposited by neutrons and photons. A double-walled vacuum vessel made of Inconel 718 and cooled by a FLiBe cooling channel, which flows between the two layers (the so called inner and outer vacuum vessels), separates the plasma from the breeding blanket. For a more detailed description of ARC components, see [1]. Finally, a layer made of beryllium and supported by the outer vacuum vessel, acts as a neutron multiplier in order to increase the TBR of ARC.

The *nemoFOAM* tool [2] has been developed inside the OpenFOAM environment [3] to perform the multi-physics analysis of nuclear (fission and fusion) systems, with the solution of the multi-group neutron diffusion equations, the monokinetic photon diffusion equation and their coupling with a thermal-hydraulic module, which takes as an input the neutronic and photonic power previously evaluated. The multi-group diffusion is an approximation with respect to the results obtained with Monte Carlo codes like Serpent [4], which has been previously employed to develop the neutronic model of ARC [5], but it allows to dramatically reduce the computational time of the simulation and to avoid issues of bad statistics far from the neutron source. The neutronic and

photonic modules of *nemoFOAM* require the definition of some multi-group nuclear and atomic properties, which can be evaluated through a preliminary Serpent simulation. Serpent computes the nuclear properties in the universes defined by the user, which in this case correspond to the main components of ARC (i.e. inner vacuum vessel, cooling channel, neutron multiplier, outer vacuum vessel and breeding blanket).

To be more accurate, these multi-group properties are associated with probability distributions which arise from the uncertainties of the nuclear data, which will affect thermal-hydraulic quantities like the temperature and the pressure drops in ARC components in terms of such uncertainties. In this work, the nuclear data uncertainties are propagated from the nuclear libraries to the nuclear properties generated by Serpent, employing non-intrusive uncertainty propagation techniques like the Total Monte Carlo (TMC). The propagation of the photonic data uncertainties has not been considered here because the main data libraries available do not contain covariance matrices for the photon data, which are necessary for the uncertainty propagation.

Other techniques, like the Unscented Transform (UT) [6] and the Polynomial Chaos Expansion (PCE) [7], allow to reduce the dimension of the input problem through the truncation of the covariance matrix and, as a consequence, the number of simulations required for the uncertainty propagation is generally smaller than TMC. However, the so-called *curse of dimensionality* makes it impossible to apply the PCE when the dimension of the input is huge, like in the case of uncertainty propagation from the nuclear data libraries. On the other hand, when the dimension of the input space is smaller, like in multi-group diffusion, the PCE can be appealing since it can be used to evaluate not only the mean and the standard deviation of the responses of interest, but also their distribution and their sensitivity to the different uncertain inputs. Thus, the PCE, together with the UT, can be a suitable choice for the uncertainty propagation from the group constants generated with Serpent to the thermal-hydraulic outputs calculated with *nemoFOAM*.

2. THE MODELS IN THE nemoFOAM CODE

In the case of a non-fissile system like ARC, the multi-group neutron diffusion equation solved by *nemoFOAM* is:

$$\frac{1}{v_g}\frac{\partial \Phi_g(\mathbf{r},t)}{\partial t} - \nabla \cdot (D_g \vec{\nabla}\Phi_g(\mathbf{r},t)) =$$

$$= -\Sigma_{abs,g}\,\Phi_g(\mathbf{r},t) + \sum_{g'=1}^{G,g\neq g'} (\Sigma_{scat,g'->g}\Phi_{g'}(\mathbf{r},t)) - \sum_{g'=1}^{G,g\neq g'} (\Sigma_{scat,g->g'}\Phi_g(\mathbf{r},t)) + S_g(\mathbf{r},t) \qquad (\forall g = 1,...,G),$$

$$(1)$$

where g represents the g-th energy group, G the total number of energy groups, D the diffusion coefficient, S an external source of neutrons and $\Phi_g(\mathbf{r},t)$ the neutron scalar flux. For what concerns the absorption (Σ_{abs}) and scattering (Σ_{scat}) terms, it is mandatory to employ the so called reduced absorption cross section and the scattering multiplication matrix provided by Serpent, in order to take also into account the contribution of (n,2n), (n,3n), etc. multiplication reactions [8]. This is particularly important in a system like ARC, where a beryllium layer is foreseen specifically for neutron multiplication. The reduced absorption cross section is defined as:

$$\Sigma_{abs} = \Sigma_{tot} - \Sigma_{scat} - \Sigma_{(n,2n)} - \Sigma_{(n,3n)} + ..., \tag{2}$$

which, by definition, can have negative values, meaning that, when there is a strong neutron multiplication effect, it can act as a source term.

Serpent has been employed also for the generation of the photon properties. The main limitation of this approach is that Serpent does not allow to generate the photon scattering matrix. To overcome this issue, as an initial approximation, the following monokinetic photon diffusion equation has been implemented in *nemoFOAM*:

$$\frac{1}{v} \frac{\partial \Phi_\gamma(\mathbf{r}, t)}{\partial t} - \nabla \cdot (D_\gamma \vec{\nabla} \Phi_\gamma(\mathbf{r}, t)) = -\Sigma_{abs,\gamma} \, \Phi_\gamma(\mathbf{r}, t) + \nu_\gamma \Sigma_{tot,n} \Phi_n(\mathbf{r}, t)) + S_\gamma(\mathbf{r}, t), \tag{3}$$

$$D_\gamma = \frac{1}{3\Sigma_{tot,\gamma}}. \tag{4}$$

The absorption attenuation coefficient, $\Sigma_{abs,\gamma}$, is given by the sum of photoelectric and pair production attenuation coefficients and $\Sigma_{tot,\gamma}$ is obtained by the sum of absorption and scattering (i.e. Compton plus Rayleigh scattering) attenuation coefficients. The neutron diffusion equation is "one-way"-coupled with the photon one by the term $\nu_\gamma \Sigma_{tot,n} \Phi_n$ which takes into account the photon production by neutrons. Φ_n is the neutron total flux. Finally, in this preliminary version of the photonic module, the photons produced by charged particles through atomic relaxation, Bremsstrahlung and annihilation are considered as an external fixed source ($S_\gamma(\mathbf{r}, t)$). All these terms have been evaluated with Serpent in each component of ARC.

For what concerns the boundary conditions for the solution of the problem, in *nemoFOAM* it is possible to employ vacuum, albedo, non-zero incoming current boundary condition and interface boundary conditions, both for the neutronic and photonic modules.

After having solved the neutronic and photonic problem, the thermal-hydraulic module of *nemoFOAM* solves the continuity equation, the Navier-Stokes' equations for the momentum and the energy conservation equation. The source term in the energy conservation equation consists of the power deposited by neutrons and photons, evaluated starting from the scalar fluxes computed with Equation (1) and Equation (3) and the kerma coefficients estimated with Serpent. In a previous work [5], it was proven that the contribution of photons to the power deposition in fusion systems like ARC is not negligible, so it must be considered in a multiphysics analysis. The numerical solution of these equations allow to evaluate quantities like temperature and pressure in the breeding blanket of ARC.

In principle, *nemoFOAM* is able to take into account also the thermal feedback on the neutronic and photonic properties, allowing to have a full coupling between the three modules, but this feature has not been taken into account in this work, also because it is expected that in a fusion system the thermal feedback is less significant than in fission reactors, where the feedback directly impacts on the fission process (i.e. the main source of neutrons in fission devices). On the other hand, in fusion reactors, the plasma (i.e. the main source of neutrons in fusion devices) is totally independent of the nuclear properties and of the temperature of the system components. In the absence of the coupling of the thermal feedback, a shorter computational time of the simulation is obtained.

3. UNCERTAINTY QUANTIFICATION METHODS

This section provides a synthetic description of the uncertainty quantification methods employed in this work, namely the Total Monte Carlo and the Unscented Transform, leaving PCE for further developments.

3.1. Total Monte Carlo

The Total Monte Carlo (TMC) method [9] allows to evaluate the distributions and, as a consequence, the mean value and the standard deviation of responses of interest in Serpent due to the uncertainties in the nuclear data. This method requires the generation of a large set of perturbed nuclear data files and a Serpent simulation for each set. If the statistical error of the Monte Carlo simulation is sufficiently small, the uncertainty of the responses resulting from the uncertain nuclear data can be inferred from the output distributions.

In this work, the responses of interest are the neutronic group constants generated by Serpent and the nuclear data have been extracted from the ENDF-B/VIII.0 library [10]. The SANDY Python package [11] has been used for the perturbation of the nuclear data, assuming that the perturbed data can be represented by correlated normal distributions.

3.2. Unscented Transform

The basic principle of the Unscented Transform (UT) [6] is to estimate the mean value and the variance of the responses distributions through the approximation of the input distribution rather than the model. In general, this idea is justified by the fact that the approximation of the input distribution is usually easier than acting on non-linear models.

The approximation of the input is obtained by the generation of a set of so-called *sigma points* that capture the essence of the input data distribution. When the aim of the uncertainty quantification is the evaluation of the first two moments of the response distribution, $2k+1$ sigma points are sufficient to get a reliable representation of the input, where k corresponds to the dimensions of the input perturbed data. In this case, k is equal to $n_G n_{GC} n_U$, where n_G is the number of energy group considered in the multigroup diffusion model in *nemoFOAM*, n_{GC} is the number of perturbed group constants and n_U is the number of universes employed in Serpent to generate the group constants. Since k can easily become very large, suitable reduction techniques, like the one applying the Low Rank Approximation (LRA) to the Singular Value Decomposition (SVD) [12], are of particular interest.

When generating the *sigma*-points, values smaller than 0 may be obtained. Since the sigma points in this work correspond to the group constants, in order to avoid non-physical negative values, a possible solution is to employ a variant of the UT, called the General Constrained Sigma Point (GCSP) method [13]. This method allows to generate all the sigma points inside the range $[0,+\infty)$, with the lower and upper limits respectively defined as μ_L, which in this case corresponds to 0, and μ_R, which in this case corresponds to $+\infty$. According to the GCSP method, the sigma points are defined as:

$$\chi^{[0]} = \mu$$
$$\chi^{[i]} = \mu + d_i \left(\sqrt{\hat{C}} \right)_i \quad \text{for } i = 1, ..., k \tag{5}$$
$$\chi^{[i]} = \mu - d_i \left(\sqrt{\hat{C}} \right)_{i-k} \quad \text{for } i = k+1, ..., 2k,$$

where:

$$d_i = \min\left(\sqrt{(k+\lambda)}, d_{i1}, d_{i2}\right),$$

$$d_{i1} = \min|\mu_U - \mu_j| / \left|\left(\sqrt{\hat{C}}\right)_{j,i}\right|, \tag{6}$$

$$d_{i2} = \min|\mu_L - \mu_j| / \left|\left(\sqrt{\hat{C}}\right)_{j,i}\right|.$$

The matrix $\hat{C} \in \mathbb{R}^{k \times k}$ is the covariance of the input, μ is the mean vector of the input and λ is an arbitrary spreading parameter (in this work, $\lambda = 1/2$ accordingly to [14]), j and i indicate the j-th row and i-th column of the matrix. The UT method requires also the computation of a set of weights, which in the GCSP are computed as:

$$\omega^{[0]} = \frac{1}{2d_i^2} \tag{7}$$

$$\omega^{[i]} = 1 - \sum_{i=1}^{2t} \omega^{[i]} \quad \text{for } i = 1, ..., 2t.$$

Then, the sigma points are passed to the model $\mathcal{M}'$ to get a set of responses, which are used to estimate the weighted mean and weighted covariance of the response distribution as:

$$\mu' = \sum_{i=0}^{2k} \omega^{[i]} \mathcal{M}'(\chi^{[i]}), \tag{8}$$

$$\hat{C}' = \sum_{i=0}^{2k} \omega^{[i]} (\mathcal{M}'(\chi^{[i]}) - \mu')(\mathcal{M}'(\chi^{[i]}) - \mu')^T, \tag{9}$$

where the index i corresponds to the i-th sigma point and weight.

When the covariance matrix is symmetric and positive semi-definite, its square root can be computed with the SVD,

$$\hat{C} = V\Sigma V^T \tag{10}$$

$$\sqrt{\hat{C}} = V\Sigma^{1/2}. \tag{11}$$

where the matrix Σ is a diagonal matrix composed by the singular values (SV) of $\hat{C}$.

Moreover, since the singular values constitute a monotonically fast-decreasing series of values, the SVD factorisation can be truncated without much approximation, moving from r positive SV to t, where t is the number of SV retained after the truncation. Consequently, the truncation allows to decrease the number of sample points from $2k+1$ to $2t+1$ and, thus, the computational time required by uncertainty propagation.

The SVD-UT algorithm followed in this work starts with the results of the TMC simulations, from which the mean μ and the covariance matrix $\hat{C}$ are obtained. The application of the SVD and LRA algorithms allows to extract a truncated square root of the covariance matrix, which is then employed to generate a specific set of perturbed group constants. These data are then passed to *nemoFOAM*, which produces a set of output responses used to estimate their mean and covariance (i.e. the error arising from the nuclear data uncertainties).

4. RESULTS

In this section we present part of the results obtained so far for what concerns the nuclear data uncertainty propagation in ARC.

4.1. Group constants generation

Serpent can be used for the generation of the group constants and, as already mentioned, these quantities are affected by the nuclear data uncertainties. In the case of UT the result of the uncertainty propagation procedure is the mean and the standard deviation of each group constant, meaning that the distribution for the group constants used in *nemoFOAM* is assumed as Gaussian. A more accurate alternative, at the cost of a more expensive calculation, is to propagate the nuclear data uncertainties in Serpent through the TMC, in order to find the exact distribution of the group constants, as shown in Figure 1, for the diffusion coefficient (D), the absorption cross section (Σ_{abs}), the kerma coefficient (kerma) and the scattering matrix (Σ_{scat}) in the FLiBe cooling channel of ARC. These distributions have been obtained randomly sampling the covariance matrix of ^{19}F using the CSWEG-239 group structure and generating 500 perturbed nuclear data files accordingly. The energy grid employed to generate the group constants in Serpent is reported in Table 1: the grid is finer for higher energies and coarser for thermal energies, consistently with typical fusion reactors spectra.

Table 1: Energy grid employed for the group constants generation in the ARC model.

Energy groups	1	2	3	4	5	6
Upper limit [MeV]	2.0E+01	1.0E+01	1.0E+00	1.0E-01	1.0E-02	1.0E-04
Lower limit [MeV]	1.0E+01	1.0E+00	1.0E-01	1.0E-02	1.0E-04	1.0E-11

The Kolmogorov-Smirnov (KS) test has been employed, suggesting that some of the distributions in Figure 1 are not Gaussian. See, as a reference, the last column in the row of the diffusion coefficient in Figure 1, where it is clear that the corresponding Gaussian distribution built starting from the mean value and the standard deviation (black curve) is different from the actual distribution (red histogram). This may happen because Serpent is a non-linear code, so it is possible to obatain non-Gaussian outputs starting from Gaussian inputs. Thus, in some cases it is important to use higher order techniques (like TMC), because using lower order, linear techniques (e.g. UT) assumes Gaussian outputs. Table 2 shows the uncertainties, due to the nuclear data, of the group constants generated for the cooling channel and the breeding blanket of ARC for the two most energetic groups. The resulting uncertainties are non-negligible and much higher than the statistical uncertainties coming from the Monte Carlo simulation (smaller than 0.1% for all the results in Table 2), underlining the importance of propagating them through *nemoFOAM*, either with the UT or the PCE, with an appropriate reduction of the input dimensionality.

In order to speed up the 500 TMC simulations for the generation of the group constants, it has been noted that it is not necessary to employ the actual ARC geometry model defined through CAD files, but it is sufficient to define a simplified toroidal geometry with the characteristic layers thicknesses of ARC. In fact, the properties computed with the two geometries are similar. In this way, the use of the constructed solid geometry (CSG) approach and of simple surfaces (i.e. tori)
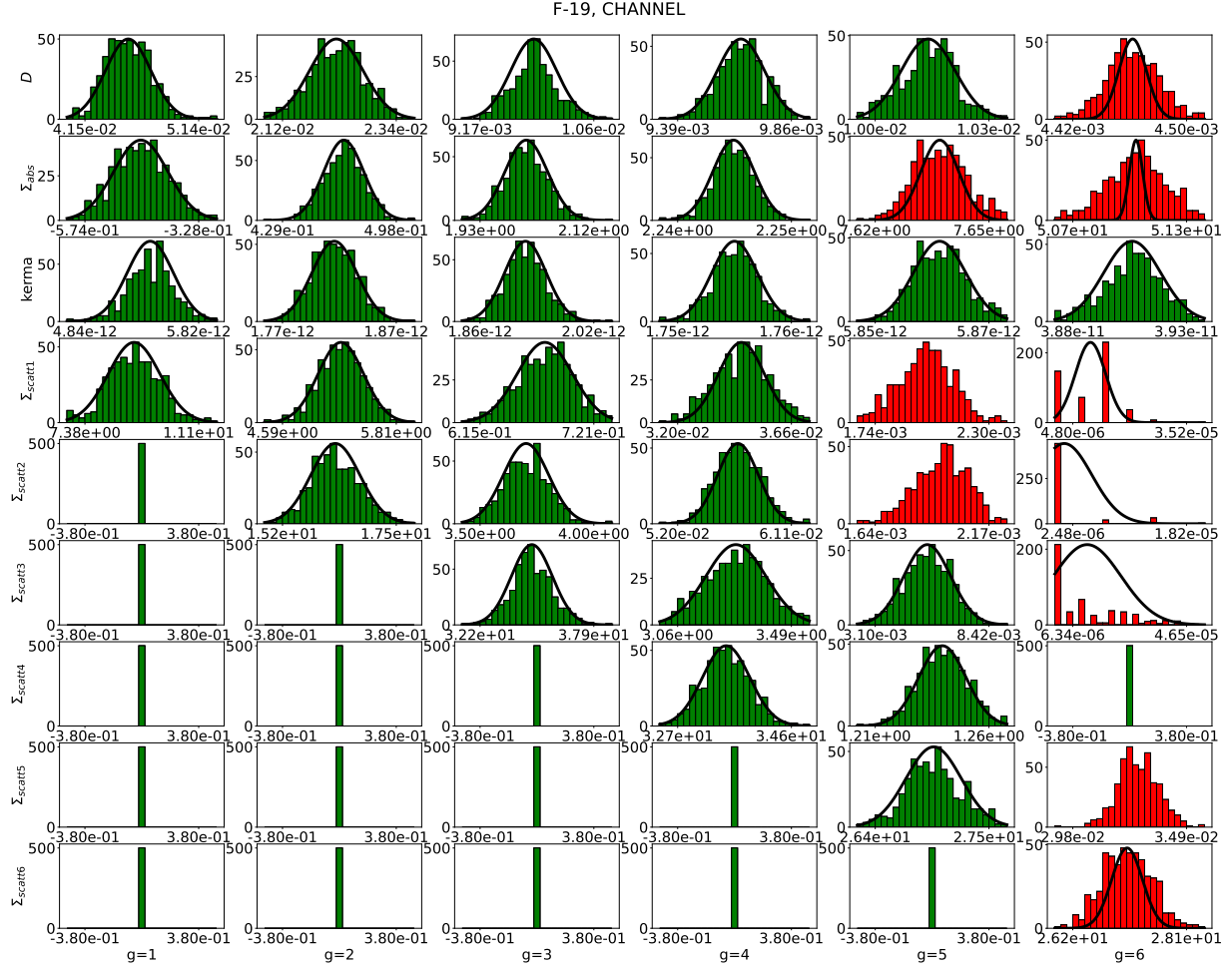
Figure 1: Distribution of the most significant group constants in the cooling channel of ARC obtained perturbing ^{19}F, using TMC. Color legend: green, the KS test suggests a Gaussian distribution; red, the KS test suggests a non-Gaussian distribution.

implemented in Serpent allows to reduce the computational time of each simulation for the group constants simulations to 2 minutes, employing $6 \cdot 10^6$ neutron histories divided in 60 batches and using 32 CPUs. This simplified geometry has been employed to reproduce the results in Figure 1.

4.2. Uncertainty propagation in *nemoFOAM*

Then, the UT has been applied starting from the probability distributions of the 500 Serpent simulations obtained perturbing ^{19}F nuclear data. In this case n_{G} corresponds to the 6 energy groups. The group constants (n_{GC}) considered are the diffusion coefficients, the reduced absorption cross sections, the scattering multiplication matrix and the kerma coefficients. Finally, the n_{U} is limited to the channel and the breeding blanket, since the major impact of the ^{19}F perturbations is located in these two universes, as displayed in Table 2. In fact, it can be observed that the impact of ^{19}F in terms of uncertainties on the group constants of the outer vacuum vessel (considered here as representative of all the components which does not contain ^{19}F in ARC) is generally much smaller.

7

Table 2: Relative standard deviation of the group constants in the cooling channel, the breeding blanket and the outer vacuum vessel of ARC, due to the nuclear data uncertainties of ^{19}F.

	$\text{RSD}_{\text{D}}[\%]$	$\text{RSD}_{\Sigma_{\text{abs}}}[\%]$	$\text{RSD}_{\text{kerma}}[\%]$
Cooling channel			
Energy group 1	4.35	12.95	3.71
Energy group 2	2.32	2.61	1.00
Breeding blanket			
	$\text{RSD}_{\text{D}}[\%]$	$\text{RSD}_{\Sigma_{\text{abs}}}[\%]$	$\text{RSD}_{\text{kerma}}[\%]$
Energy group 1	4.23	14.30	3.55
Energy group 2	2.30	2.93	1.21
Outer vacuum vessel			
	$\text{RSD}_{\text{D}}[\%]$	$\text{RSD}_{\Sigma_{\text{abs}}}[\%]$	$\text{RSD}_{\text{kerma}}[\%]$
Energy group 1	0.00	7.93	0.12
Energy group 2	0.07	0.73	0.76

This has allowed to limit the total number of input parameters to 108. Truncating the covariance matrix at an energy of 99.997%, further reduces the number of singular values to 23, meaning 47 neutronics and thermal-hydraulics simulations with *nemoFOAM*, instead of 217.

The 47 *nemoFOAM* simulations have been performed in steady state conditions using 24 CPUs and requiring around 7 hours per simulation (of which around 30-40 minutes for the neutronic and photonic part). The results of a preliminary neutronic, photonic and thermal-hydraulic simulation have been used as initial guess in order to speed up the convergence of the 47 computations.

Table 3 shows the uncertainties on the total power deposition (neutrons and photons) due to the uncertainties of ^{19}F nuclear data in the main components of ARC. It can be noticed that relative errors are significantly higher in the components which contain ^{19}F (i.e. the cooling channel and the breeding blanket), as expected. Another interesting result is that, in general, the relative errors are comparable with the ones obtained with Serpent in [14], which can be considered as the reference results.

Table 3: Relative uncertainty on the total power deposition in ARC computed with *nemoFOAM* due to ^{19}F, using UT.

	Inner vacuum vessel	Cooling channel	Neutron multiplier	Outer vacuum vessel	Breeding blanket
Power [MW]	29.87 ± 0.07	81 ± 1	21.73 ± 0.09	51.1 ± 0.1	256 ± 3
Error [%]	0.231	1.51	0.416	0.359	0.967

Table 4 shows the uncertainties on thermal-hydraulic responses of interest, like the maximum temperature in each component and the pressure drop between the inlet and the outlet of the FLiBe

circuit in ARC. Here, the results are referred to the *Channel+Breeding blanket* since the cooling channel and the breeding blanket have been considered as a single region in the thermal-hydraulic model. In this case the uncertainties are much smaller because the nuclear data uncertainties have an indirect impact on temperature and pressure drop through the neutron power deposition which, conversely, is directly affected by the nuclear data uncertainties. Such small values do not seem to represent a concern for the design of ARC and they suggest to take into account also other nuclides in future analysis, like ^{58}Ni. ^{58}Ni could have a larger impact on the maximum temperature of the vacuum vessel, since it is the nuclide present with the higher percentage in this component.

Table 4: Relative uncertainty on the maximum temperatures and on the pressure drop in ARC computed with *nemoFOAM* due to ^{19}F, using UT.

	Inner vacuum vessel	Neutron multiplier	Outer vacuum vessel	Channel+ Breeding blanket
T_{max} [K]	891.5 ± 0.3	885.3 ± 0.3	929.5 ± 0.4	895 ± 1
Error [%]	0.0360	0.0307	0.0481	0.149
Δp [bar]	5.427 ± 0.002			
Error [%]	0.0303			

5. CONCLUSIONS

In this work, the Total Monte Carlo method has been employed to propagate the nuclear data uncertainties of ^{19}F from ENDF-B/VIII.0 data library to the group constants generated by Serpent in ARC. Then, the distributions obtained through the TMC have been exploited in order to propagate the effect of the uncertainties on thermal-hydraulic quantities through the OpenFOAM solver *nemoFOAM* using the Unscented Transform method. The results suggest that the impact of ^{19}F uncertainties on temperatures and pressure drop is probably not the major source of uncertainties in ARC. In the future, other nuclides like ^{58}Ni should be analysed, since it is possible that its impact on the maximum temperature of the vacuum vessel can be non-negligible. A similar procedure can be applied also to thermo-physical properties, since they are generally evaluated through experiments and, by definition, have uncertainties. Moreover they directly impact on the thermal-hydraulic responses, so a larger effect of their uncertainties can be expected.

Finally, the number of inputs required by *nemoFOAM* is still too high to obtain reliable results with PCE in a reasonable computational time. However, it will be interesting to test the PCE with the neutronic module of *nemoFOAM*, since it requires a significantly smaller amount of computational time with respect to the thermal-hydraulic one, in order to obtain the probability distributions of the neutronic power deposition in ARC.

REFERENCES

[1] B. Sorbom, J. Ball, T. Palmer, F. Mangiarotti, J. Sierchio, P. Bonoli, C. Kasten, D. Sutherland, H. Barnard, C. Haakonsen, J. Goh, C. Sung, and D. Whyte. "ARC: A compact, high-field, fusion nuclear science facility and demonstration power plant with demountable magnets." *Fusion Engineering and Design*, **volume 100**, pp. 378 – 405 (2015).

[2] M. Caravello. *Multiphysics analysis of ARC blanket.* Master's thesis, Politecnico di Torino (2022). URL http://webthesis.biblio.polito.it/id/eprint/24295.

[3] H. G. Weller, G. Tabor, H. Jasak, and C. Fureby. "A tensorial approach to computational continuum mechanics using object-oriented techniques." *Computers in Physics*, **volume 12**(6), pp. 620–631 (1998). URL https://aip.scitation.org/doi/abs/10.1063/1.168744.

[4] J. Leppänen, M. Pusa, T. Viitanen, V. Valtavirta, and T. Kaltiaisenaho. "The Serpent Monte Carlo code: Status, development and applications in 2013." *Annals of Nuclear Energy*, **volume 82**, pp. 142–150 (2013).

[5] A. Aimetta, N. Abrate, S. Dulla, and A. Froio. "Neutronic Analysis of the Fusion Reactor ARC: Monte Carlo Simulations with the Serpent Code." *Fusion Science and Technology*, **volume 78**(4), pp. 275–290 (2022). URL https://doi.org/10.1080/15361055.2021.2003151.

[6] S. J. Julier and J. K. Uhlmann. "New extension of the Kalman filter to nonlinear systems." In I. Kadar, editor, *Signal Processing, Sensor Fusion, and Target Recognition VI*, volume 3068, pp. 182 – 193. International Society for Optics and Photonics, SPIE (1997).

[7] D. Xiu and G. E. Karniadakis. "The Wiener–Askey polynomial chaos for stochastic differential equations." *SIAM journal on scientific computing*, **volume 24**(2), pp. 619–644 (2002). URL https://doi.org/10.1137/S1064827501387826.

[8] J. Leppänen, M. Pusa, and E. Fridman. "Overview of methodology for spatial homogenization in the Serpent 2 Monte Carlo code." *Annals of Nuclear Energy*, **volume 96**, pp. 126–136 (2016). URL https://www.sciencedirect.com/science/article/pii/S0306454916303899.

[9] A. Koning and D. Rochman. "Towards sustainable nuclear energy: Putting nuclear physics to work." *Annals of Nuclear Energy*, **volume 35**, pp. 2024–2030 (2008). URL https://www.sciencedirect.com/science/article/pii/S0306454908001813.

[10] D. Brown and M. C. et. al. "ENDF/B-VIII.0: The 8th Major Release of the Nuclear Reaction Data Library with CIELO-project Cross Sections, New Standards and Thermal Scattering Data." *Nuclear Data Sheets*, **volume 148**, pp. 1–142 (2018). URL https://www.sciencedirect.com/science/article/pii/S0090375218300206. Special Issue on Nuclear Reaction Data.

[11] L. Fiorito, G. Žerovnik, A. Stankovskiy, G. Van den Eynde, and P. Labeau. "Nuclear data uncertainty propagation to integral responses using SANDY." *Annals of Nuclear Energy*, **volume 101**, pp. 359–366 (2017). URL https://www.sciencedirect.com/science/article/pii/S0306454916305278.

[12] B. Foad, A. Yamamoto, and T. Endo. "Efficient uncertainty quantification for PWR during LOCA using unscented transform with singular value decomposition." *Annals of Nuclear Energy*, **volume 141**, p. 107341 (2020). URL https://www.sciencedirect.com/science/article/pii/S0306454920300396.

[13] D. Li and Y. Wang. "Constrained unscented Kalman filter for parameter identification of structural systems." *Structural Control and Health Monitoring*, **volume 29**(4), p. e2908 (2022). URL https://onlinelibrary.wiley.com/doi/abs/10.1002/stc.2908.

[14] A. Aimetta, N. Abrate, S. Dulla, and A. Froio. "A Nonintrusive Nuclear Data Uncertainty Propagation Study for the ARC Fusion Reactor Design." *Nuclear Science and Engineering*, **volume 0**(0), pp. 1–25 (2023). URL https://doi.org/10.1080/00295639.2022.2153638.